MEASUREMENT OF CHARGED PARTICLE INTERACTIONS IN SPACECRAFT AND PLANETARY HABITAT SHIELDING MATERIALS

Cary J. Zeitlin,[1*] Lawrence H. Heilbronn,[1] Jack Miller,[1] John W. Wilson,[2] Robert C. Singleterry Jr.[2]

Lawrence Berkeley National Laboratory,[1] NASA Langley Resarch Center[2]

Abstract

Accurate models of health risks to astronauts on long-duration missions outside the geomagnetosphere will require a full understanding of the radiation environment inside a spacecraft or planetary habitat. This in turn requires detailed knowledge of the flux of incident particles and their propagation through matter, including the nuclear interactions of heavy ions that are a part of the Galactic Cosmic Radiation (GCR). The most important ions are likely to be iron, silicon, oxygen, and carbon. Transport of heavy ions through complex shielding materials – including self-shielding of tissue – modifies the radiation field at points of interest (e.g., at the blood-forming organs). The incident flux is changed by two types of interactions: (1) ionization energy loss, which results in reduced particle velocity and higher LET (Linear Energy Transfer); and (2) nuclear interactions that "fragment" the incident nuclei into less massive ions. Ionization energy loss is well understood, nuclear interactions less so. Thus studies of nuclear fragmentation at GCR-like energies are needed to fill the large gaps that currently exist in the database. These can be done at only a few accelerator facilities where appropriate beams are available. Here we report results from experiments performed at the Brookhaven National Laboratory's Alternating Gradient Synchrotron (AGS) and the Heavy Ion Medical Accelerator in Chiba, Japan (HIMAC).

Recent efforts have focused on extracting charge-changing and fragment production cross sections from silicon beams at 400, 600, and 1200 MeV/nucleon. Some energy dependence is observed in the fragment production cross sections, and – as in other data sets – the production of fragments with even charge numbers is enhanced relative to those with odd charge numbers. These data are compared to the NASA-LaRC model NUCFRG2. The charge-changing cross section data are compared to recent calculations using an improved model due to Tripathi, which accurately predicts the observed (slight) energy dependence.

An additional set of data will be presented from an analysis of shielding material performance in the 1 GeV/nucleon iron beam at the AGS. A wide variety of candidate materials for spacecraft construction, as well as elemental targets, have been placed in this beam and their effects on transmitted dose and dose equivalent measured. The results support a prediction by J. Wilson et al. that hydrogen-loaded materials give the greatest dose reduction per unit mass.

Introduction

Three broad categories of space radiation are simulated in experiments performed by our group at ground-based particle accelerators: High-energy protons and ions (HZE) in the Galactic Cosmic Radiation (GCR); medium-energy protons from the GCR and from Solar Particle Events (SPE); and low-energy

trapped protons. In terms of absorbed dose, these are the most important particle types encountered by humans in space. GCR-like particle beams can be obtained at the AGS and HIMAC; medium-energy protons are available at the Loma Linda University Proton Treatment Center; and low-energy protons at energies approximating trapped protons are produced at the Lawrence Berkeley National Laboratory's 88" Cyclotron. In all of these categories, experimental data obtained by our group provide checks on model calculations, particularly those of the NASA-LaRC group, whose codes are used in spacecraft and spacesuit shielding models.

The experiments and calculations described here fall under two headings: fundamental physics relevant to the development of transport codes, and shielding materials studies. In the former category, we include measurements of cross sections for charged-particle production in HZE reactions [1, 2, 3] using elemental targets. The data obtained in these experiments are used for comparison to transport models, for example, the NASA-LaRC code NUCFRG2 [4] and others. The ultimate aim of the measurements is to fill in many of the holes in the existing database of cross sections for nucleus-nucleus interactions, which should lead to improvements in the semi-empirical portions of the transport codes. The second category of experiments, the shielding materials studies, includes iron-beam fragmentation measurements [5] using composite targets, performed primarily at the AGS.

Charged-particle Cross Sections in HZE Reactions
In these experiments, HZE ions at GCR-like energies are produced at the AGS and HIMAC, and elemental targets are placed in the path of the beam. The targets used are C, Al, Cu, Sn, Pb, and, in some recent experiments, a Li target has been used. Polyethylene (CH_2) is also; when cross sections obtained with the C target are subtracted from those with polyethylene, one obtains the cross sections on H, which are of particular interest for two reasons. First, and most relevant here, calculations [6] predict that hydrogenous materials provide superior shielding. Second, pertinent to astrophysics, the observed GCR flux is the result of transport from the sources through the interstellar medium, which is primarily hydrogen. Thus, accurate measurements of H-target cross sections are needed if the GCR composition at the source is to be understood.

The experiments described here use silicon detectors placed along beam axis (0°). Detectors are placed so as to subtend varying acceptance angles, as illustrated schematically in Fig. 1. Many data sets have been obtained at 0º, and a few data sets have been obtained with detectors placed off the beam axis, in order to make direct measurements of fragment angular distributions. The existing data on angular distributions are quite sparse.

Spectra obtained at 0° are used to extract the charge-changing and fragment production cross sections (σ_{cc} and σ_Z), which depend on the species of the beam and target nuclei, and on the beam energy. Over the range of energies pertinent to the GCR, energy dependence of the cross sections is observed to be mild. As shown in Figure 2, significant differences are seen in spectra obtained with detectors placed at large acceptance (i.e., near the target exit, as in Fig. 2a) compared to spectra obtained with detectors further downstream (Fig. 2b). These differences give indirect information about fragment angular distributions. We note that virtually all previously published 0° measurements used only large acceptance detectors, and did not report cross sections for light fragments.

The spectrum in Fig. 2a illustrates the reason for the lack of light-fragment cross sections from earlier experiments: at large acceptance, there are simply no well-resolved fragment peaks below approximately

half the beam charge, making particle identification at the low end impossible. This is a consequence of the relatively high multiplicity of fragments produced when the incident beam ion undergoes a central collision and is broken up into many lighter nuclei. Because light fragments have relatively broad angular distributions, many of them are outside the acceptance of detectors placed far downstream of the target (i.e., at small acceptance). The reduction in observed multiplicity produces very clean spectra like the one in Fig. 2b. Note that although the fragment multiplicity is reduced at small acceptance angles, there are nonetheless several peaks in Fig. 2b that can only be explained by the presence of at least two fragments detected in coincidence, e.g., the peak near $Z = 3.5$, which is likely due to events in which three He fragments are detected. Other multiple-fragment peaks appear as shoulders just above the single-fragment peaks at 4, 5, 6, and 7. Another notable feature of Fig. 2b is the peak of approximately 3000 events (out of about 300,000 total) at $Z = 0$; these are events in which all the charged fragments were outside the acceptance of this detector.

Once the Z spectra are produced, a simple count of the numbers of events detected as a function of species is the main input to the calculation of the charge-changing and fragment production cross sections. Fig. 2 shows that even-charged fragments are preferentially produced, resulting in enhanced fragment production cross sections for those species, as illustrated in Fig. 3. The production of F ($Z = 9$) is particularly suppressed. Details such as these provide sensitive tests of models of nuclear interactions.

Charged-particle Fluences Behind Thick Targets
In a series of accelerator experiments similar to the cross-section measurements, we have placed thick, usually composite targets in the path of heavy ions beams. Most of our data have been acquired with the 1087 MeV/nucleon ^{56}Fe beam at the AGS. Fluence spectra have been obtained for many targets. Because the beam energy is relatively high, effects of fragmentation predominate over ionization energy-loss effects. Thus, in this beam, for any target material, the dose per particle exiting the target will be decreased relative to the dose per particle of the incident beam ions, provided the areal density is less than about 20 g cm^{-2}. (Especially at lower energies, there is a tradeoff between the two: Energy loss tends to increase LET and hence dose per particle, for those particles with sufficient energy to traverse the full depth of the target; fragmentation reactions, on the other hand, reduce the nuclear charge, reduces the dose per particle.) Despite this general trend, variations are still seen when we quantify the reduction in dose per particle reduction with different shielding materials.

The analysis of these data is simple. Starting with the LET of the 1087 MeV/nucleon AGS ^{56}Fe beam (148 keV/μm), using target-out data we determine a scale factor to convert the measured quantity (deposited energy, ΔE, in silicon) to LET. This factor is then applied to convert ΔE distributions acquired with targets in the beam to LET spectra. In a manner similar to that employed in the cross-section data analysis, we obtain counts of fragments and surviving primaries by species and apply (small) corrections for losses in the detector. The corrected counts are then used to obtain a corrected average LET, $<L>$, which with this beam is invariably lower than the beam LET, L_{beam}. Because the targets are of modest depth and the beam energy is high, there are essentially no particles stopped in the target, and therefore (in the simplest approximation), the fluence exiting the target is equal to the incident fluence. Therefore $<L>$ is directly proportional to the dose of the mixed field seen behind the target. For each target, we compute the fractional dose reduction per unit mass, given by $f = (1 - <L> / L_{beam})/(\rho * x)$ where $\rho * x$ is the areal density of the target. Results are shown below in Fig. 4.

710

In [6], Wilson *et al.* predict that hydrogenous materials will, in the space radiation environment, give the best performance per unit mass in terms of both dose equivalent and cell transformation probability. The results in Fig. 4, though not directly comparable, are qualitatively consistent with this prediction: the greatest dose reductions are seen with the Epoxy and Boron-Epoxy targets, which are hydrogen-rich. The Martian regolith simulant target also does well; it too has considerable hydrogen content (it consists of polyethylene blended with a mixture that approximates Martian soil). The smallest dose reductions are seen for elemental targets, Cu and Al (Pb data are also available but have not yet been analyzed for this purpose). Many more data sets have been obtained that can be applied to this analysis. Varying the beam ion and energy will provide a broader test of the relative performance of the different materials.

Summary

Extensive charged-particle measurements with GCR-like ions have been made for purposes of improving the nuclear cross section database and for direct measurements of shielding properties of various materials. Though considerable progress has been made in recent years, a large archive of data still awaits analysis and publication.

References

1. C. Zeitlin, L. Heilbronn, J. Miller, S. E. Rademacher, T. Borak, T. R. Carter, K. A. Frankel, W. Schimmerling, and C. E. Stronach, *Phys. Rev.* C **56**, 388 (1997).
2. C. Zeitlin, A. Fukumura, L. Heilbronn, Y. Iwata, J. Miller, T. Murakami, *Phys. Rev.* C **64**:024902 (2001).
3. C. Zeitlin, A. Fukumura, L. Heilbronn, Y. Iwata, J. Miller, T. Murakami, LBNL Report Number 47655 (2002).
4. J. W. Wilson, J. L. Shinn, L. W. Townsend, R. K. Tripathi, F. F. Badavi, S. Y. Chun, *Nucl. Instr. Meth.* B **94**, 95 (1994).
5. J. Miller, C. Zeitlin, L. Heilbronn, F. A. Cucinotta, LBNL Report Number 49423 (2002). Accepted for publication in *Radiation Research*.
6. J. W. Wilson, M. Kim, W, Schimmerling, F. F. Badavi, S. A. Thibeault, F. A. Cucinotta, J. L. Shinn, and R. Kiefer, *Health Phys*. **68**, 50 (1995).
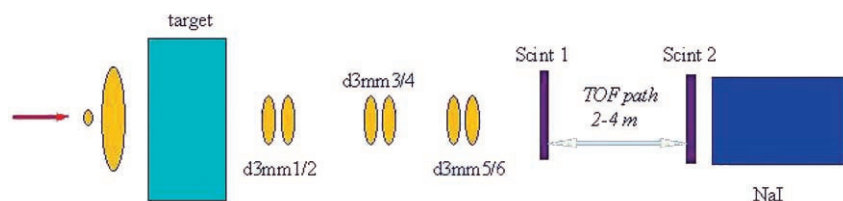
Figure 1. Schematic layout of charged-particle experiments at HIMAC. At the AGS, the TOF (time-of-flight) is not used due to the limited space available along the beamline.
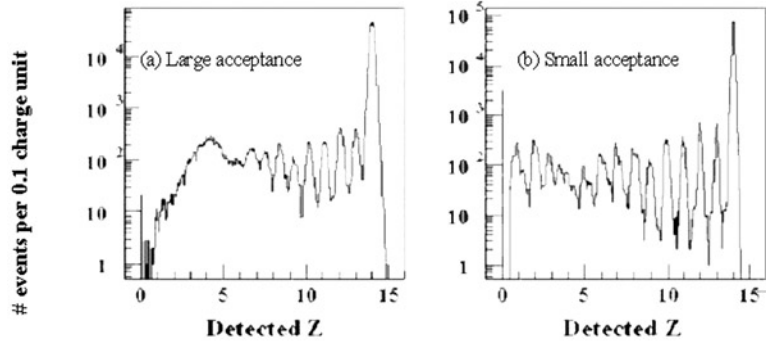
Figure 2. Spectra obtained with the 600 MeV/nucleon ^{28}Si beam at HIMAC incident on a 1.31 g cm^{-2} carbon target.
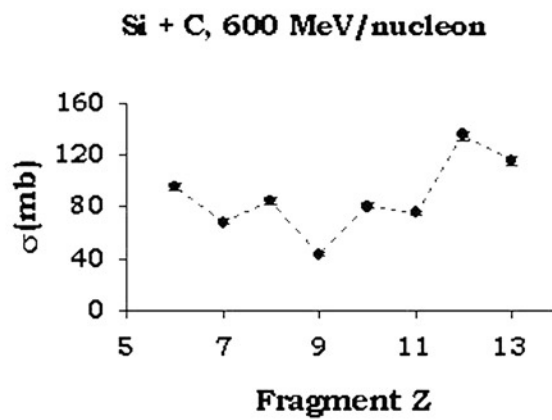

Figure 3. Fragment production cross sections for ^{28}Si on carbon at 600 MeV/nucleon, showing the "odd-even" effect (enhanced production of even-Z fragments).
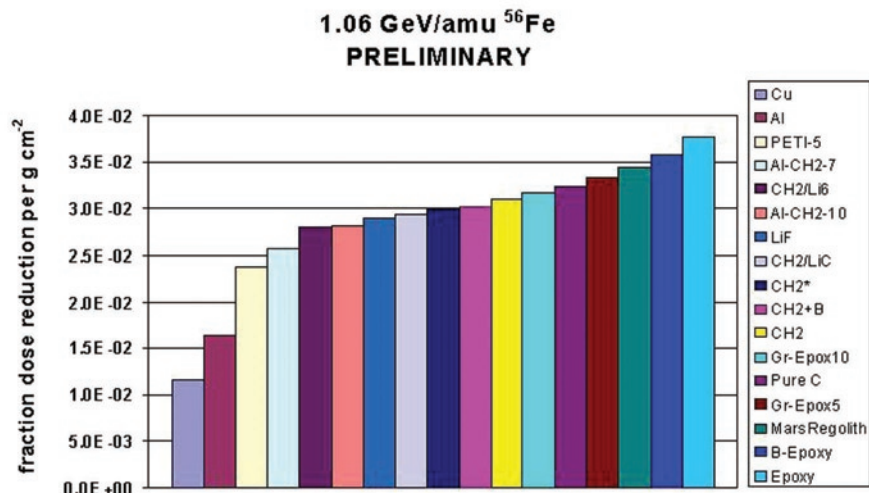

Figure 4. Dose reductions for various materials placed in the 1087 MeV/nucleon ^{56}Fe beam at the AGS. The list of target names in the legend, starting at the top, corresponds to the entries in the chart from left to right (i.e., the left-most chart entry is for the Cu target, followed by Al, PETI-5, etc.).